A Modular, Distributed, Soft, 3-Axis Sensor System for Robot Hands

Tito Pradhono Tomo, Wai Keat Wong, Alexander Schmitz, Harris Kristanto,
Alexandre Sarazin, Lorenzo Jamone, Sophon Somlor and Shigeki Sugano, *Fellow, IEEE*

***Abstract*— Integrating distributed sensors in the skin of robot hands is challenging, as the space is limited. This paper presents a dense and small tactile sensor system that can be installed on robotic hands. In the current implementation, the system is constituted by modules that are 26mm long and 27mm wide and they have been successfully integrated on the internal side of each finger phalange of the commercially available Allegro Hand (except the fingertips). Each sensor module contains 16 tri-axial taxels; each taxel is able to measure the applied 3D force vector using a Hall effect sensor and a magnet. The sensor modules are 4mm high, including the printed circuit board (PCB) with the sensors and the soft silicone with the magnets. The back of the PCB is flat without any components mounted, which eases the integration. Each sensor has I2C digital output, and each sensor module is connected to four I2C buses, requiring only seven wires for each module. The tri-axial taxels are close to each other (4.7 mm from the center of one taxel to the next), but experiments proved that independent force vectors can be measured and that the crosstalk is limited.**

I. Introduction

Human-symbiotic robots that are supposed to work with and like humans benefit from a soft and sensitive skin, to enhance their safety and their object handling skills. Especially grippers or hands are supposed to be often in contact with the environment; the human hand has one of the highest density of tactile sensors in the human skin. Integrating distributed tactile sensors in the multi-fingered hands of robots is challenging, as the space is limited. Not only the space for the transducers, but also for the wires and the digitization electronics needs to be taken into account. Distributed tactile sensors have been integrated into several robotic hands, for example [1][2][3]. A common limitation is that only single axis force can be measured, or if the force vector can be measured, only one force vector for each finger phalange can be obtained.

The capability to measure a distributed force vector is crucial for dexterous object handling and provides rich haptic information about the manipulated objects. Since the individual tri-axial taxels are very small and close to each other, the proposed sensor allows to precisely retrieve i) the points of contact, ii) the 3D force vector at each point of contact, iii) the overall shape of the area of contact, iv) the overall 3D force vector applied to the area of contact. Interestingly, the sensor deals well with cases in which multiple contacts points are simultaneously present on the same module: this is a typical problematic situation for current state of the art tri-axial force sensors.

The current paper introduces distributed tactile sensors for the phalanges of the Allegro hand. Each module is 26mm long, 27mm wide and 4mm high; each module can measure 16 force vectors with 16 3-axis Hall effect sensors. The output of each module is digital and requires only seven wires. The back of the sensor modules is flat so that they can be attached to the Allegro hand straightforwardly. The sensor modules incorporate silicone (2mm – 3.5mm thick, depending on the location); softness for robot skin has been shown to be beneficial for safety and object handling. Furthermore, in addition to the 16 force vector measurements, each module also has eight 3-axis accelerometers and all 24 sensors also measure temperature. Therefore, the modules also provide multimodal information. These features expand the potential applications of this sensor for not only force control, ensuring grasp stability and for tactile servoing, but also for classifying the surface texture and enhanced tactile object recognition. This paper focuses on the Hall effect sensors to measure the distributed 3-axis force vector. Experiments were performed to evaluate the crosstalk of the Hall effect sensors.

In previous work [4] our lab has introduced a soft and distributed 3-axis force sensor based on capacitive sensing, but each 3-axis force measurement required 14x14x7 mm, and the production was time-consuming. In comparison, the current sensor requires much less space and the production is easy. In [5][6] the prototype Hall effect sensor to measure a single 3-axis force vector was introduced; the drift due to temperature and a compensation algorithm using the integrated temperature sensor, minimal detectable normal force, and 3-axis calibration were discussed. The current paper introduces sensor modules with 16 3-axis force vector measurements that are ready for the integration in the robot hand and evaluates the distributed force vector measurements.

The rest of this paper is organized as follows. In Section II we provide a review of related tactile sensors. Section III describes the sensor principle, the production process and the integration into the Allegro hand. Section IV presents the experimental procedure that was used to evaluate the sensor and shows the results. Section V draws conclusions and presents future work.

II. Related Works

The literature describes many tactile sensors [7][8], but few of them of them can measure multi-axis force and can or have been integrated into robotic hands. Several robot hands, for example [1][3], have 3- or 6-axis F/T sensors integrated into their fingertips, usually based on strain gauges; the MAC

Tito Pradhono Tomo, Wai Keat Wong, Alexander Schmitz, Harris Kristanto, Alexandre Sarazin, Sophon Somlor and Shigeki Sugano are with Waseda University, Tokyo, Japan (corresponding author e-mail: tito@toki.waseda.jp)

Lorenzo Jamone is with the Instituto de Sistemas e Robótica, Instituto Superior Técnico, Lisbon, Portugal (e-mail: ljamone@isr.tecnico.ulisboa.pt)

hand [9] and Robonaut 2 hand [10] have such sensors also in the other finger phalanges. Only one force vector per finger segment can be obtained. Tri-axial sensors also based on strain gauges were integrated into the soft skin of the robot Macra [11], but these sensors would be too big for distributed sensing in robot hands.

Small sized transducers can be produced with MEMS. For example, in [12] a thin sensor based on strain gauges is described. A robotic fingertip with 4 tri-axial sensors is presented in [13], and Touchence[1] sells a thin 3-axis tactile sensor based on piezoelectric elements. Yet, the necessary additional electronics are bigger than the sensor itself.

Optical sensors using cameras can obtain multi-axis force with a high resolution [14][15][16] and have been integrated into the fingertips of grippers, but would be too thick for thin robot skin. A small-sized optical 3-axis sensor was proposed more than ten years ago in [17], but not investigated further. The optical 3-axis sensor in [11] has been integrated into soft sensor flesh and is commercially available by Touchence as well. A smaller (10mm wide and 8mm high) optical tri-axial sensor is currently available from OptoForce[2].

In [18][19] a bump was added on top of an array of four capacitive sensors to make the array sensitive to shear forces; a tiltable plate above the sensors was used in [20]. Capacitive skin sensors that can measure the shear forces without a bump or plate are suggested in [21][22], but the skin does not include the measurement electronics. Therefore, the use for distributed sensing in robotic skin is not straightforward. A capacitive 3-axis sensor with digital output and embedded in soft silicone is presented in [4].

The idea of using Hall effect sensors and magnets to measure a tactile response was originally proposed in [23] and [24], where only preliminary prototypes were presented, and then not investigated anymore until recently [25]-[29]. The sensors in [27][28] are integrated into a robot hand, but only normal forces can be measured. The work in [25] instead proposes a 3D sensor, but the sensors were not used for distributed sensing. The work described in [26] and [29] has been successfully applied to real robotic scenarios; however, the design they proposed (with a rubber dome and four Hall effect sensors) imposed constraints on the minimum size of the whole system. A magnetic based tactile sensor for fingertips has been commercially produced[3]. However, the output signal from this sensor has to be amplified first before a microcontroller can read it. The amplifier has a significant size, meaning that a lot of space is required for integrating this device into a robot.

In summary, tactile sensors that can measure the force vector are commonly too big to be integrated in thin skin and/or they need additional bulky electronics, which makes the integration of distributed sensors in a robot challenging.

III. Sensor Description

The sensor described in this paper is easy to produce. This section describes the sensor structure as well as the production process.

[1] http://www.touchence.jp
[2] http://optoforce.com/
[3] http://bl-autotec.co.jp/

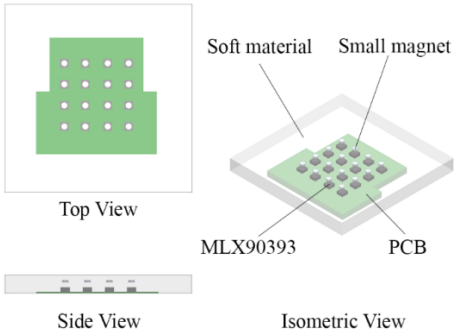

Fig. 1 Conceptual design.

A. Sensor Concept

In previous research [5] we developed the first prototype of a Hall effect based skin sensor with a single MLX90393 chip and successfully detected normal and shear forces. A single chip can provide 3-axis magnetic data and temperature data. A small magnet is placed above the chip, and the movement of the magnet can be acquired by measuring the magnetic field change, which corresponds to the 3-axis force.

For the integration into a robot hand, especially for the purpose of in-hand manipulation, a distributed force measurement is beneficial. For this reason, we improved the skin sensor by developing a custom PCB mounted with 16 Hall effect sensor chips. The chips were distributed within a 26mm x 27mm area, placed 4.7mm apart from each other as shown in Fig 1. 16 small magnets were embedded above the chips. A deformable material such as silicone is necessary to create a layer between the chip and the magnet.

The MLX90393 has I2C fast mode protocol (4-wire). Each chip has a 7-bit address, and the last 2 bits can be configured by connecting the corresponding pin to either the power source or ground. For this reason, one data line (SDA) can share four chips at the same time. Four SDA lines are required to acquire force measurements from 16 chips. One module has seven cables including VCC (+3.3V), GND, SCL, and four SDAs for communicating with a microcontroller. We used a multiplexer or I2C splitter with PCA95448A from BitWizard connected to the Arduino Due's SDA port.

B. Manufacturing Process

Fig. 2 shows the manufacturing process for the distributed skin sensor. First, the custom PCB with 16 MLX90393 chips was placed in the middle of a molding cast. The guidance lid (Fig. 2 (a)) for making 16 holes was placed on the top of it, ensuring the holes were placed in the center of each chip. Afterwards, enough liquid silicone rubber was poured for the silicone to cover all the PCB and touch the lid. After the silicone had cured, the lid was removed, leaving 16 small holes. 16 small magnets were placed inside the holes, floating about 1mm above the chips. The magnet for the current implementation was neodymium (grade N50) with a 1.69mm diameter and a 0.53mm thickness. It had an optimal pull of 226.8g and 729 surface gauss. After the magnets had been placed inside the holes, more liquid silicone rubber was poured to cover the magnets with silicone. The overall thickness of the silicone layer above the PCB is 3.5mm.

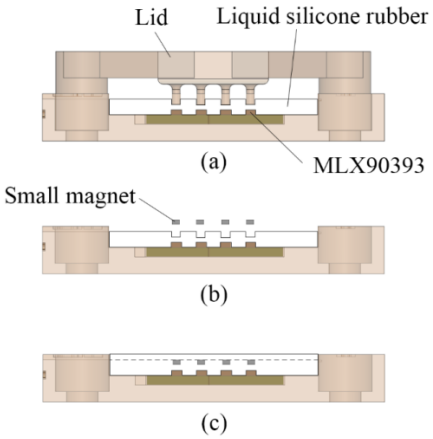

Fig. 2 The molding process. (a) Liquid silicone rubber was poured into the molding cast. (b) 16 small magnets were placed inside the hole. (c) Another layer of liquid silicone rubber was poured above the magnets.

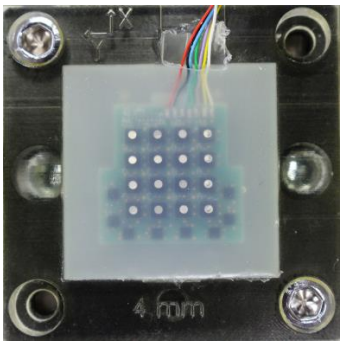

Fig. 3 A distributed skin sensor embedded with 16 MLX90393 chips, providing 48 force data in total.

Considering the thickness of the chip (1mm) and the magnet, the silicone has a thickness of at least 2mm. The prototype of the proposed sensor can be seen in Fig. 3.

The silicone material used in this research is Ecoflex Supersoft from Smooth-On, shore hardness 00-30, which is softer than human skin. Please note that an optimal material selection is not the focus of this paper. The ideal hardness depends on the application and encountered force limits; Ecoflex Supersoft 30 proved to provide reasonable results considering sensitivity and range for a robot hand. Furthermore, softness in general is beneficial for safety and object handling, as described in the introduction, yet causes problems for the sensor characteristics. Therefore, Ecoflex Supersoft 30 was purposely chosen, to test how the sensor works in a soft skin. Ecoflex Supersoft 10 is even softer with a shore hardness of 00-10, but has an oily film on the surface even after curing.

C. Integration in the robot hand

The sensor modules fit on the motors that constitute the phalanges of the fingers of the Allegro hand, as shown in Fig. 4. Another silicone mold compared to the one shown in the last section was used to create the silicone shown in Fig. 4, which surrounds the fingers of the Allegro hand. The thickness of the sensor module including a 0.5mm thick PCB is 4mm. The connections between the finger phalanges have

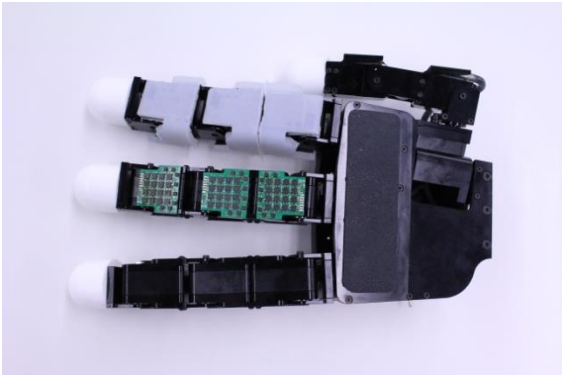

Fig. 4 An Allegro Hand integrated with our proposed sensors (middle) and covered with skins (top).

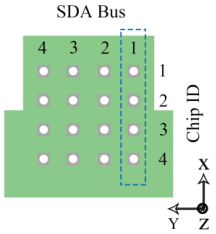

Fig. 5 SDA bus and chip ID assignment for the skin sensor. SDA 1 was selected for the experiments.

to be made 4mm longer than in the original hand in order for the fingers being able to bend without touching the sensors, thereby extending the length of the finger 12mm in total. Finally, while for the current experiments we use rather bulky electronics to collect the I2C measurements, small sized microcontrollers are available; for example, the microcontroller board used for the skin sensors in iCub is about 26x18x6mm big, can collect measurements from four I2C buses, and is connected on a daisy chain CAN bus.

Since a servo motor is installed in each joint, we considered that the magnetic field from the motor may interfere with the skin sensor readout. However, after conducting a test by activating the servo motors while the skin sensor was mounted, the result revealed that there was no magnetic field interference. The skin sensor reading was not affected by the rotation of the motor.

IV. Evaluation

Three experiments were conducted to evaluate the performance of the skin sensor. In the first experiment the measurment of normal and shear force is tested; the second experiments investigates the crosstalk between the chips. In the third test we repeatedly push the sensor, to test it stability. SDA 1 was selected for the experiments, see Fig. 5.

A. Experimental Setup

Fig. 6 shows the test setup. The test setup consists of a current controlled (without force feedback) voice coil motor (VM5050-190 from Geeplus) to apply normal force, a linear bushing, an aluminum shaft adapter, a 6-axis force/torque (F/T) sensor (Nano 1.5/1.5 from BL autotech) for monitoring the pushing force, and a 12x12mm 3D printed push plate with a flat surface. The load limit for the F/T sensor is 15N for the x, y and z axis, respectively. Therefore, in our experiments

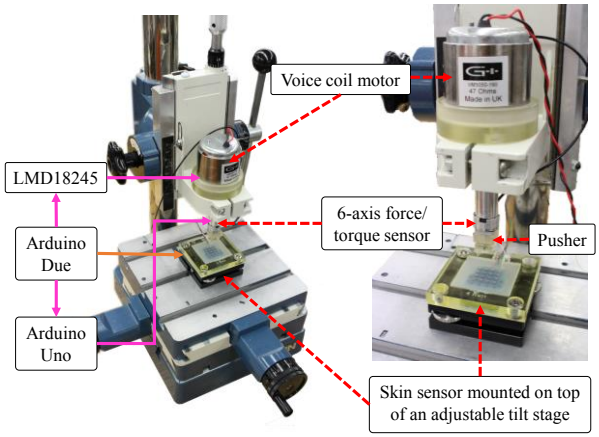

Fig. 6 Experiment setup used in this paper.

the maximum load applied per axis is kept below 15N. The orientation of the skin sensor was fine adjusted with a tilt stage to achieve a parallel contact with the push plate. We used an LMD18245 from Texas Instrument for changing the load force by controlling the current to the voice coil motor. The F/T sensor and our sensor required 5V and 3.3V supply voltage, respectively. For this reason, we used two microcontrollers, Arduino Uno and Due. They were synchronized, and both data were recorded on SD cards with a sampling rate of 40Hz. The skin sensor was mounted on a sturdy X-Y table; the position where to apply the force can be adjusted with the X-Y table; also shear force can be applied by moving the X-Y table after an initial contact with the push plate. Unfiltered sensor data was used for all experiments and is shown in the plots.

B. Sensor Measurements before Calibration

Fig. 7 shows the result of the load test when a normal force was applied centered above a sensor. Before the calibration, as shown in Fig. 7 (a), our skin sensor shows some displacements in the x-axis (S_x, marked as blue) and y-axis (S_y, marked as green) even though only normal force was applied, see Fig. 7 (b). A possible reason for this is that the placement of the magnet was not perfectly centered, and due to the incompressibility of the silicone, causing a small sideward displacement of the magnet if it is not perfectly centered initially. We discovered a similar situation in Fig. 8., which shows combined shear and normal force.

C. Calibration

Load was applied to the sensor by stepwise increasing and subsequently decreasing the force on a single chip. The sensor was calibrated with data when applying force only in the x, y or z axis, respectively. In particular, three kinds of force (normal, shear in the x-axis, and shear in y-axis) were applied on the top of each sensor once each, resulting in three time series data to calibrate each Hall effect sensor. When applying force only in the z-axis, each step lasted 5s and the force was changed by changing the reference voltage of the LMD18245 in steps of 0.27V. In total 21 steps were performed for increasing and decreasing the force, and at step 11 the maximum force of around 14N was achieved. When applying force in either the x or y axis, each step lasted 6 seconds; a

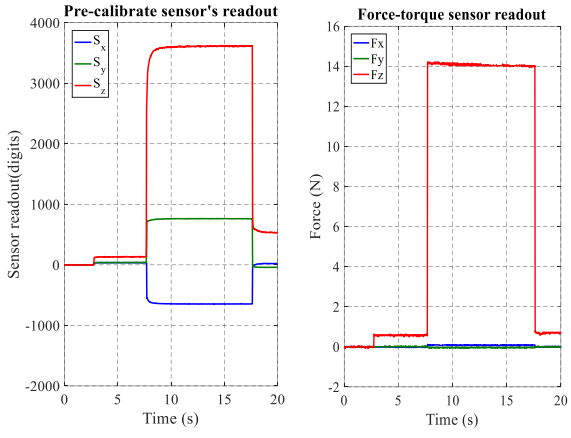

Fig. 7 The sensor's readout (a) and the corresponding force from F/T sensor (b) when only the normal force is applied (chip 4 SDA1).

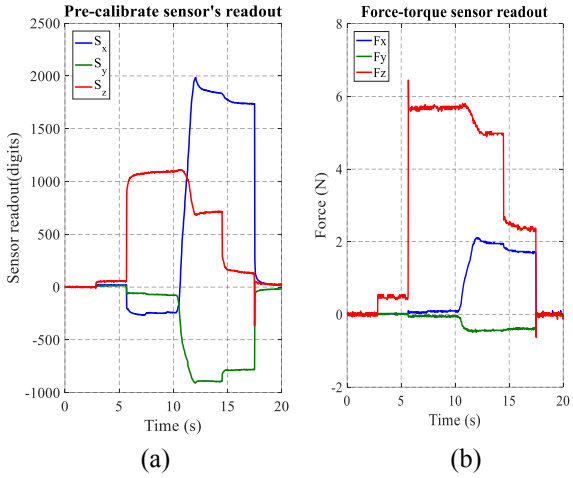

Fig. 8 The sensor's readout (a) and the corresponding force from the F/T sensor (b) when shear force is applied (sensor 3 SDA1).

longer time interval was chosen because the force was applied manually by moving the X-Y table, which requires about 1s. For each step, the X-Y table was moved 0.5 mm by turning the fine adjuster knob of the X-Y table. Overall, 10 steps were performed. Each taxel was calibrated independently. We used the MATLAB Curve Fitting Toolbox™, and a quadratic model with a robust Huber regression for calibrating the sensor. We removed 15 samples before and after each load change to clean the dataset from unwanted transient signals. We found that the prediction performance for test data increased when cleaning the training data in such a way. For each chip, all 3 sensor measurements are used to calculate each force in the x, y and z-axis, therefore 6 parameters for each axis have to be calculated for each chip.

For testing, we used data that was not used for calculating the calibration parameters. Fig. 9 shows a representative result when only normal force was applied, while Fig. 10 displays the calibrated sensor measurements when also shear forces in the x-axis and y-axis were applied, respectively. For Fig. 10, the load was changed every 6 seconds: first the z-load was automatically changed every 6 seconds, and immediately afterwards for each step the shear force was changed manually.

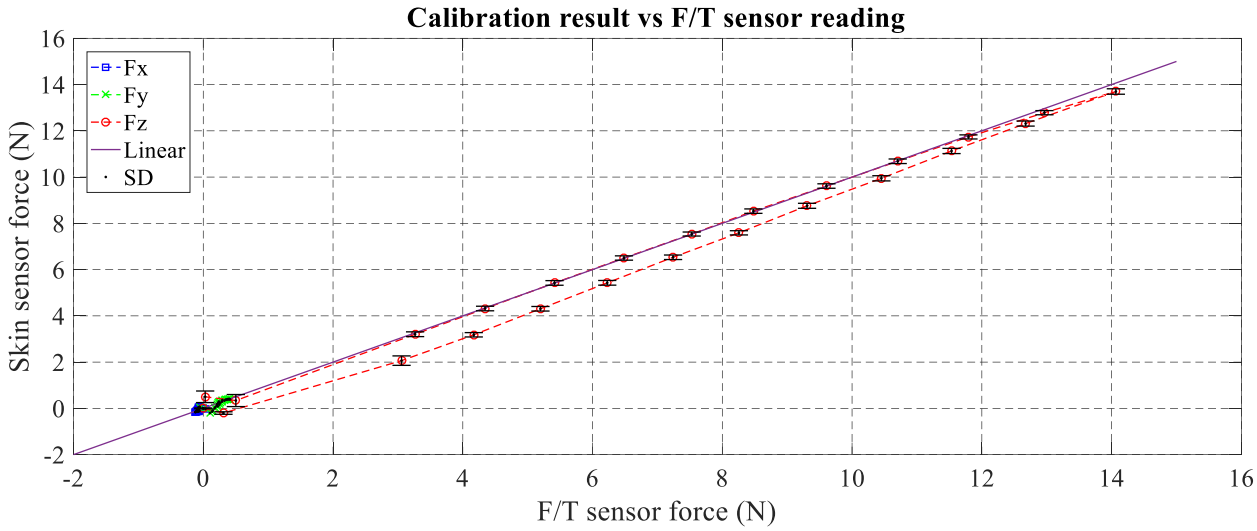

Fig. 9 Calibrated sensor response when normal force is applied (chip 3 SDA1).

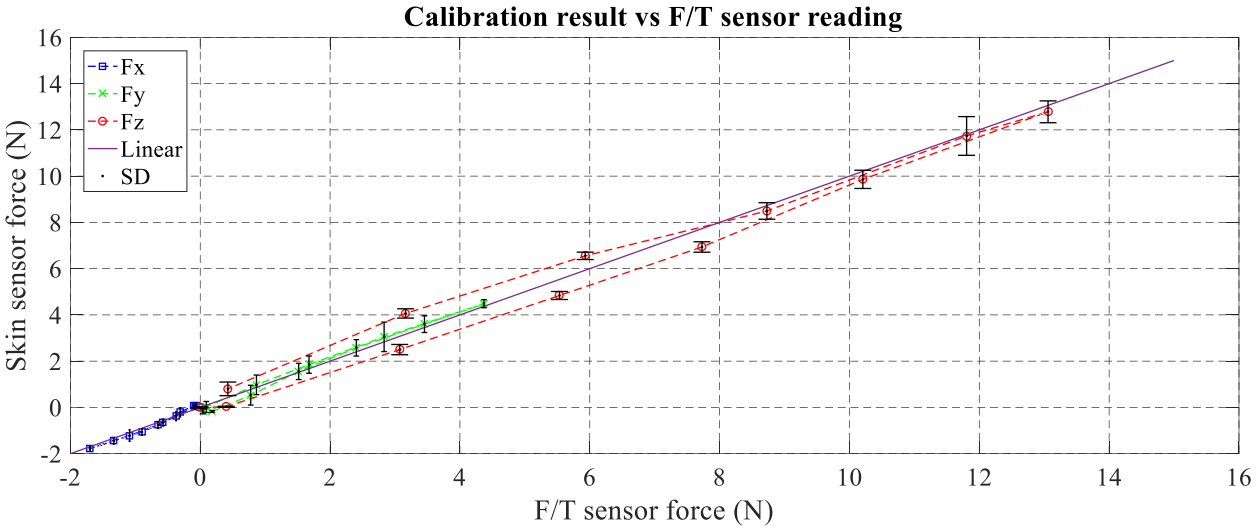

Fig. 10. Calibrated sensor response when normal and shear force are applied (chip 4 on SDA1).

The figures compare the mean force measured by the F/T sensor to the mean value of the calibrated skin sensor in the x, y, and z-axis, respectively, for every step. Also the standard deviation (SD) for the skin sensor for each step is shown. Fig. 11 presents a zoom on the x-axis and shows that the sensor is sensitive also to low forces.

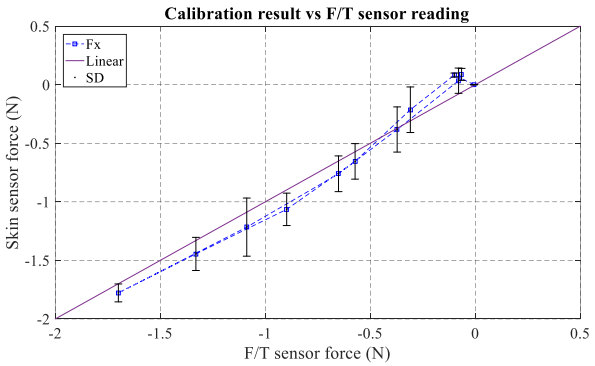

Fig. 11. Calibrated sensor response when shear force is applied. (Sensor 4 on SDA1, x-axis only).

The calibrated skin sensor readout displays a similar value as the F/T sensor readout. This result verifies that the skin sensor can measure normal and shear forces. The R-squared values from the calibration results can be seen in Table 1. R-squared value represents how close the data are to the fitted regression line. The hysteresis of the normal force load test was 5.29 %, calculated using equation 1.

$$Hysteresis \quad \% = \left| \frac{(F_{mu} - F_{ml})}{(F_{\max} - F_{\min})} \right| \times 100\% \qquad (1)$$

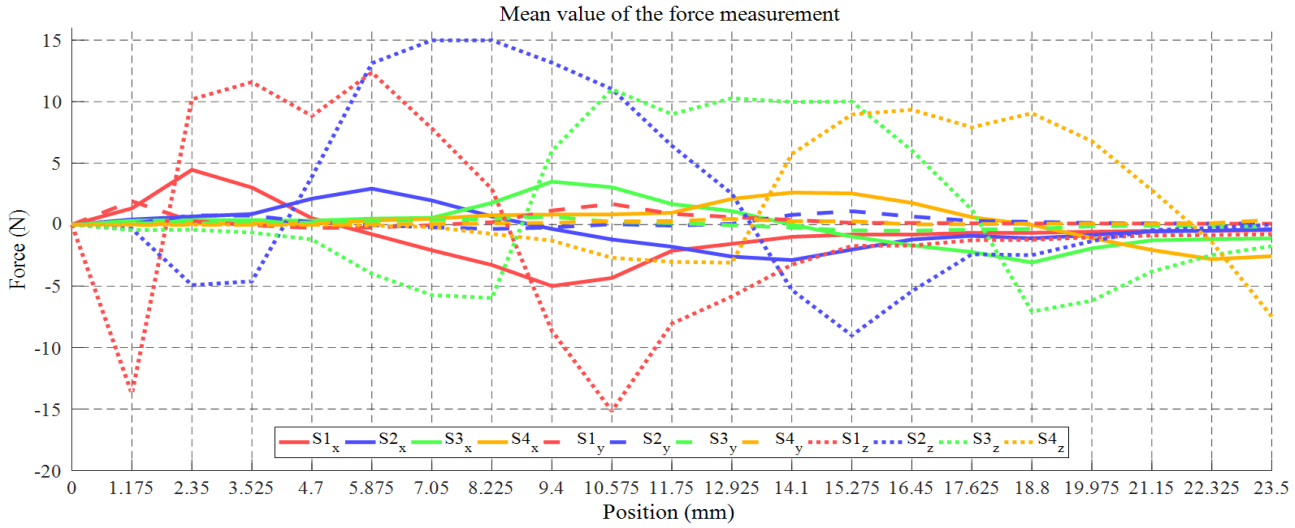

Fig. 12 The average force value of individual sensor on all positions.

F_{ml} and F_{mu} are the calibrated skin force values (linear interpolation of the nearest neighbors) of the loading and unloading cycles, respectively, taken at the midpoint force of (14N – 0N)/2 = 7N. F_{min} was the mimimally measured average force and F_{max} the maximum measured average force.

D. Crosstalk Test

To evaluate the magnetic field interference that can affect another Hall effect sensor measurement while one chip is being pushed, a crosstalk test was conducted. Bus no. 1 was selected for this experiment. A 14N load was applied every 1.175mm (a fourth of the distance between two chips) in the x-axis, starting from -4.7mm away from the center of chip no. 1. The force was applied for around 10 seconds for each position; we waited sufficient between pushing at different positions to avoid the effect of hysteresis on this experiment. Twenty positions were recorded in total. Afterward, the mean value of the force was calculated.

Force was applied at 20 locations. Chip no. 1, 2, 3, and 4 are marked in red, blue, green, and yellow, respectively. Fig. 12 shows the average force value of each chip in all positions. The location of the chip no.1, 2, 3, and 4 is at 4.7mm, 9.4mm, 14.1mm, and 18.8mm, respectively. It can be seen that the force in z-axis increases when the contact location is closer to the magnet. In contrast, the detected force becomes weaker with increasing distance to the contact location. This result demonstrates that our proposed skin sensor can detect the force contact location.

At certain points, the force was measured as a negative value. It happened when the silicone material was pressed next to the corresponding magnet. This and the sensor measurements in the x-axis are probably due to the fact that the silicone is incompressible. Interestingly, the distance of the two peaks in the negative z-axis corresponds to the size of the pusher plate (12mm).

Chip no. 1 is slightly more sensitive in the negative z-axis direction and the chip no. 2 more sensitive in the positive z-axis direction, but overall all 4 chips show a similar response pattern. The sensor calibration was performed with less data than in the previous section (for each taxel with only 3 time series, similar to the ones shown in Fig. 7 and Fig. 8), and can probably be improved with more data.

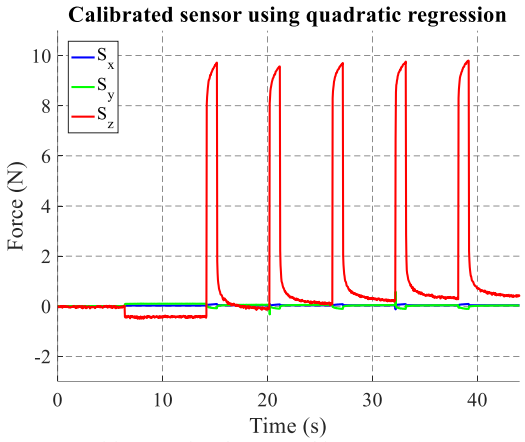

Fig. 13. Repetitive test signal output (chip 3 SDA 1).

Table 1. R-squared value for the normal force and shear force experiments

	Linear + Huber	Quadratic + Huber
Normal Force	0.9211	0.9867
Shear in x-axis	0.5286	0.9723
Shear in y-axis	0.5105	0.9836

E. Repetitive Test

To evaluate the sensor reliability, we conducted a repetitive test. In this test, we repeatedly applied a normal force of 9.8N on top of the sensor (Chip ID 4) for 1 second and retracted the pusher for 5 seconds in five cycles. The calibrated sensor output is shown in Fig. 13. The result shows that the skin sensor can reproduce a similar output during the 5 cycles. The graph also shows that the skin sensor accumulated around 0.49N load due to the hysteresis effect of the silicone.

V. Conclusion

This paper presented the design of a skin sensor with 16 Hall effect sensors. Load tests were performed by applying normal and shear forces on the proposed sensor. The tests revealed that when only normal force was applied, displacements in the x-axis and y-axis were detected. However, after performing a calibration, a similar result as the reference sensor force measurement could be achieved. The test also revealed that the shear forces in x and y-direction could be measured. Further tests were performed to measure the distributed sensor response when being pushed in different locations. It was concluded that the sensor can be used to detect the distributed force vector. In future work we want to include an air gap between the chip and the magnet to counteract the incompressibility of the silicone and its associated effects. Furthermore, grasping experiments with the hand will be performed to evaluate the sensor measurements during real use.

Acknowledgment

This research was partially supported by the JSPS Grant-in-Aid for Scientific Research (S) No. 25220005, JSPS Grant-in-Aid for Young Scientists (B) No. 15K21443, Research Institute for Science and Engineering of Waseda University, the Program for Leading Graduate Schools, "Graduate Program for Embodiment Informatics" of the Ministry of Education, Culture, Sports, Science and Technology, and Project LIMOMAN [PIEF-GA-2013-628315].

References

[1] H. Iwata and S. Sugano. Design of human symbiotic robot TWENDY-ONE. *Proc. IEEE Int. Conf. Robot. Autom.* 2009. p. 580–586.

[2] A. Schmitz, P. Maiolino, M. Maggiali, L. Natale, G. Cannata, G. Metta. Methods and technologies for the implementation of large-scale robot tactile sensors. *IEEE Trans. Robot*. IEEE; 2011;27:389–400.

[3] T. Mouri, H. Kawasaki, K. Yoshikawa, J. Takai, and S. Ito, "Anthropomorphic robot hand: Gifu Hand III," in *Proc. Int. Conf. on Control, Automation and Systems* (ICCAS), pp. 1288–1293, October 2002

[4] S. Somlor, R. S. Hartanto, A. Schmitz, and S. Sugano, "A Novel Tri-axial Capacitive-Type Skin Sensor," *Adv. Robot.*, accepted.

[5] T.P. Tomo, S. Somlor, L. Jamone, A.Schmitz, S. Hashimoto, and S. Sugano, "Development of a Hall Effect Based Skin Sensor", *Proc. IEEE Sensors Conference*, 2015.

[6] T.P. Tomo, S. Somlor, A.Schmitz, L. Jamone, W.K. Wong, H. Kristanto and S. Sugano, Design and Characterization of a 3-Axis Hall Effect Based Soft Skin Sensor, *Sensors*, 16.4 (2016): 491

[7] R.S. Dahiya, P. Mittendorfer, M. Valle, G. Cheng, V.J. Lumelsky, "Directions toward effective utilization of tactile skin: A review," *IEEE Sensors Journal*, 13 (11), 4121-4138, 2013.

[8] R.S. Dahiya, G. Metta, M. Valle, G. Sandini. "Tactile Sensing - From Humans to Humanoids", IEEE Trans. Robot. 2010;26:1–20.

[9] Cannata G, Maggiali M. An embedded tactile and force sensor for robotic manipulation and grasping. Humanoid Robot. 2005 5th IEEE-RAS Int. Conf. IEEE; 2005. p. 80–85.

[10] L.B. Bridgwater, Ihrke CA, Diftler MA, Abdallah ME, Radford NA, Rogers JM, Yayathi S, Askew RS, Linn DM. The robonaut 2 hand - Designed to do work with tools. Robot. Autom. (ICRA), 2012 IEEE Int. Conf. 2012.

[11] T. Yoshikai, M. Hayashi, Y. Ishizaka, H. Fukushima, A. Kadowaki, Sagisaka T, Kobayashi K, Kumagai I, Inaba M. Development of robots with soft sensor flesh for achieving close interaction behavior. Adv. Artif. Intell. Hindawi Publishing Corp.; 2012;2012:8.

[12] H. Takahashi, Nakai A, Thanh-Vinh N, Matsumoto K, Shimoyama I. A triaxial tactile sensor without crosstalk using pairs of piezoresistive beams with sidewall doping. Sensors Actuators, A Phys. Elsevier; 2013;199:43–48.

[13] C.M. Oddo, Controzzi M, Beccai L, Cipriani C, Carrozza MC. Roughness encoding for discrimination of surfaces in artificial active-touch. Robot. IEEE Trans. 2011;27:522–533.

[14] M. Ohka , Tsunogai A, Kayaba T, Abdullah SC, Yussof H. Advanced Design of Columnar-conical Feeler-type Optical Three-axis Tactile Sensor. Procedia Comput. Sci. 2014;42:17–24.

[15] S. Saga, Morooka T, Kajimoto H, Tachi S. High-Resolution Tactile Sensor Using the Movement of a Reflected Image. Proc. Eurohaptics. 2006. p. 81–86.

[16] W. Yuan, Li R, Srinivasan MA, Adelson EH. Measurement of shear and slip with a GelSight tactile sensor. Robot. Autom. (ICRA), 2015 IEEE Int. Conf. 2015. p. 304–311.

[17] K. Yamada, Goto K, Nakajima Y, Koshida N, Shinoda H. A sensor skin using wire-free tactile sensing elements based on optical connection. Proc. 41st SICE Annu. Conf. SICE 2002. 2002. p. 131–134.

[18] M.Y. Cheng, Lin CL, Lai YT, Yang YJ. A polymer-based capacitive sensing array for normal and shear force measurement. Sensors. 2010;10(11):10211–25.

[19] H. Lee, Chung J, Chang S, Yoon E. Normal and Shear Force Measurement Using a Flexible Polymer Tactile Sensor With Embedded Multiple Capacitors. J. Microelectromechanical Syst. 2008;17:934–942.

[20] T. Hoshi, Shinoda H. Robot skin based on touch-area-sensitive tactile element. Robot. Autom. 2006. ICRA 2006. Proc. 2006 IEEE Int. Conf. Ieee; 2006. p. 3463–3468.

[21] L. Viry, Levi A, Totaro M, Mondini A, Mattoli V, Mazzolai B, Beccai L. Flexible three-axial force sensor for soft and highly sensitive artificial touch. Adv. Mater. 2014;26:2659–2664.

[22] J.A. Dobrzynska, Gijs MAM. Polymer-based flexible capacitive sensor for three-axial force measurements. J. Micromechanics Microengineering. IOP Publishing; 2013;23:15009.

[23] J.J. Clark, "A magnetic field based compliance matching sensor for high resolution, high compliance tactile sensing," *Proceedings. 1988 IEEE Int. Conf. Robot. Autom.*, 1988.

[24] W.C. Nowlin, "Experimental results on Bayesian algorithms for interpreting compliant tactile sensing data," *Proceedings. 1991 IEEE Int. Conf. Robot. Autom.*, 1991.

[25] C. Ledermann, S. Wirges, D. Oertel, M. Mende, and H. Woern, "Tactile sensor on a magnetic basis using novel 3D Hall sensor-First prototypes and results," in *Intelligent Engineering Systems (INES), 2013 IEEE 17th International Conference on*, 2013, pp. 55–60.

[26] S. Youssefian, N. Rahbar, and E. Torres-Jara, "Contact Behavior of Soft Spherical Tactile Sensors," *IEEE Sensors Journal,* 14 (5), 1435–1442, 2014.

[27] L. Jamone, G. Metta, F. Nori, and G. Sandini, "James: A humanoid robot acting over an unstructured world," in *Humanoid Robots, 2006 6th IEEE-RAS International Conference on*, 2006, pp. 143–150.

[28] L. Jamone, L. Natale, G. Metta, and G. Sandini, "Highly sensitive soft tactile sensors for an anthropomorphic robotic hand," *IEEE Sensors Journal*, 15 (8), 4226 - 4233, 2015.

[29] E. Torres-Jara, I. Vasilescu, and R. Coral, "A soft touch: Compliant tactile sensors for sensitive manipulation," 2006.

[30] Melexis, "MLX90393 Micropower Triaxis® Magnetometer Datasheet," 2015.